Coupled Fluid-Structure Interactions Using the Fast Multipole Method

Daniel R. Wilkes (1), Alec J. Duncan (1)

(1) Centre for Marine Science and Technology, Curtin University, Perth, Australia

ABSTRACT

The interaction of sound with an arbitrarily shaped underwater object must in general be treated as a coupled interaction between the fluid and structure, due to the acoustic impedance properties of water. Typically, this type of problem is solved by building a numerical model of the exterior fluid and interior solid regions and then simultaneously solving the coupled system of equations, on the common fluid-structure interface. These models are restricted by their high cost in terms of computational time and memory. The fast multipole method (FMM) significantly reduces these requirements and is applicable to many types of boundary integral equations. For simple structures, a coupled model using the FMM for both the fluid and structure will provide a substantial increase in the possible model size or frequency limit compared to traditional methods. This paper discusses such a model and presents initial non-coupled results in the form of acoustic scattering and target strength results for the rigid BeTSSi submarine model.

INTRODUCTION

Numerical modelling methods are commonly used for analysing coupled fluid-structure interactions, as analytical solutions only exist for simple geometric shapes, such as spheres and infinite cylinders (Junger & Feit, 1993). Of the available numerical methods, the finite element method (FEM) and the boundary element method (BEM) are generally used to model the structure and fluid respectively, as they have favourable properties for modelling the corresponding domain and are amenable to coupling with one another.

The FEM is formulated using a differential equation, namely the elastic wave equation in the case of modelling displacement in an elastic solid. The 3-dimensional volume is discretised into many elements and the wave equation is posed for each, in terms of the nodal coordinates defining each element. A matrix equation is then constructed and solved for the node displacements, using appropriate boundary conditions. One advantage of using the FEM to model the interior structure is that every element may have different material properties defined by the Lame constants, allowing complex geometries involving numerous properties to be modelled.

Conversely, the BEM is derived from a boundary integral equation (BIE); the Helmholtz BIE when modelling the exterior acoustic field. In this case, the unknown variables are limited to the surface of the object, thus the discretisation only involves a 2-dimensional surface mesh. Again, a matrix equation can be constructed and solved for the surface pressure field, which in turn can be used to calculate the acoustic field at any point in the domain. This method is advantageous for modelling the fluid domain, as the exterior region is assumed infinite in size and, unlike the FEM, the BEM does not require any volume discretisation.

Coupling the fluid and structural domains described by the BEM and FEM models can be achieved by enforcing continuity conditions at the common boundary between the two domains: the pressure and the velocity normal to the surface should match on the shared boundary (Jensen et al, 2000). The force due to the acoustic pressure on the exposed surface of the finite elements can be related to the fluid pressure on the BEM surface. Similarly, the normal derivative of the surface structural displacements can be related to the normal derivative of the fluid pressure (Amini, Harris & Wilton, 1992). This casts both the FEM and BEM matrix into a form involving the pressure and displacement on the coupled surface, allowing a simultaneous solution of the coupled system of equations.

The main disadvantage of this type of coupled model is that both the FEM and BEM are limited in terms of the number of 'unknowns' which can be solved for. The BEM's restriction of the unknowns to a 2-dimensional surface reduces the total problem size, but the corresponding matrix equation is densely populated, asymmetric and complex valued (Xiao & Chen, 2007). The FEM discretises 3-dimensional space, introducing more unknowns than the BEM, but the corresponding matrix is sparse, symmetric and real valued, making it more suited to iterative solvers (Reddy, 2004). In any case, both methods require matrices of coefficients to be formed and stored, and matrix-vector multiplications to be conducted at a cost of N^2 operations for N unknowns (Gumerov & Duraiswami, 2007).

The matrices resulting from the BEM discretisation are fully populated, as the pressure at each element is calculated as the sum of contributions of every boundary element (i.e. an integral over the surface), which is implemented as a matrix-vector multiplication. The fast multipole method (FMM) can greatly expedite the calculation of the BEM interactions by determining the result of the matrix-vector calculations, without explicitly forming the matrix, and by calculating interactions between groups of elements instead of pair-wise interactions (Amini & Profit, 2003).

The FMM was originally introduced by Greengard & Rokhlin (1987) for particle interactions and later extended to the Helmholtz BIE, in 2-dimensions by Rokhlin (1990) and 3 dimensions by Coifman, Rokhlin and Wandzura (1993), for the study of electromagnetic waves. One of the first applications of the FMM to acoustic scattering appears to be by Koc & Chew (1998) where they use the FMM to accelerate the calculations for the 'T-matrix' method. Subsequently, a large volume of research has been published on the fast multipole BEM (FMBEM) for the Helmholtz equation, including 'broadband' formulations which switch between low and high

frequency expansions methods (Gumerov & Duraiswami, 2009; Cheng et al, 2006). A book on FMBEM discussing several types of BIE problems has been published by Liu (2009) while a text dealing specifically with the FMBEM for the 3-dimensional Helmholtz equation has been produced by Gumerov and Duraiswami (2004).

A more or less straightforward extension to the coupled FEM-BEM concept is to instead use the FMBEM to accelerate the BIE part of the model. Fischer and Gaul (2005) first published such a FMBEM-FEM model using a mortar-coupling method to couple the dissimilar fluid/solid meshes. A more direct coupling method was implemented by Schneider (2008) using coincident meshes, where a later study showed that this 'direct' coupling scheme is computationally superior to the former (Brunner, Junge & Gaul, 2009). This type of coupling has been extended, for example, by using half-space formulations for the fluid domain (Brunner et al. 2009) or by replacing the FEM model with a modal analysis of the structure (Masumoto et al, 2008).

A further extension to the FMBEM-FEM concept is to attempt to utilise the FMM for both the fluid *and* solid domains. Structural dynamic problems can be solved by applying the BEM to an elastodynamic BIE (in lieu of using the FEM), which allows the displacement and stress for an elastic isotropic solid to be solved using only unknowns on the surface of the solid (Beskos, 2003). As such, solid elastic models can also be treated using the FMBEM, with the first excursion into this type of model being conducted by Fujiwara (2000). Chaillat, Bonnet and Semblat (2008) presented an improved elastodynamic FMBEM which incorporated additional features of the FMM (which improve the method's performance). The same authors have shown that the elastodynamic FMBEM can also be applied to piece-wise continuous domains, using a coupled FMBEM-FMBEM formulation (Chaillat, Bonnet & Semblat 2009).

Here, a similar type of FMBEM-FMBEM formulation is proposed for coupled fluid-structure interactions, where an underwater object is modelled using the Helmholtz FMBEM for the fluid domain, and an elastodynamic FMBEM models the structure. The models will be coupled using a 'direct' coupling of surface unknowns, for coincident boundary element meshes. Current progress on the research is presented in this paper, including background theory for the BIEs of interest, details of the multi-level FMM, the proposed coupled fluid-structure model and finally acoustic scattering results from the implemented Helmholtz FMBEM. These results take the form of low frequency scattered surface pressure results for the rigid BeTSSi target strength submarine hull (compared to that from a commercial BEM software) as well as a comparison of monostatic target strength results.

BOUNDARY INTEGRAL EQUATIONS

The Helmholtz integral equation

The Helmholtz equation is a partial differential equation which represents the linear wave equation in the frequency domain (Jensen, 2000). An integral formulation can be obtained from Green's second identity using the pressure p and the Helmholtz free-space solution, or Green's function:

$$G(\mathbf{x},\mathbf{y}) = \frac{e^{ikr}}{4\pi r} \tag{1}$$

where $r = |\mathbf{x} - \mathbf{y}|$ is the radial distance between the source position $\mathbf{x}$ and receiver position $\mathbf{y}$ and k is the wavenumber (Wu, 2000). It can be seen that the Green's function has the form of a spherically radiating point source and exhibits a singular nature as $r \to 0$. A limiting process can be applied to Green's second identity where it can be shown that the volume integrals cancel out and the resulting integral, in the limiting case as a source approaches the boundary, becomes:

$$-\frac{1}{2}p(\mathbf{y}) = \int_S \frac{\partial p(\mathbf{x})}{\partial n(\mathbf{x})} G(\mathbf{x},\mathbf{y}) dS(\mathbf{x}) - \int_S p(\mathbf{x}) \frac{\partial G(\mathbf{x},\mathbf{y})}{\partial n(\mathbf{x})} dS(\mathbf{x}) \tag{2}$$

where S is the boundary surface and the partial derivatives of the pressure and Green's function are taken with respect to the outward pointing normal of the surface, at the source position $\mathbf{x}$ (Gumerov, 2009). The minus sign on the left hand side is for exterior acoustic problems (positive for interior problems) and the ½ comes about from the general case of $\mathbf{y}$ being located at a smooth point on the surface, for which the ratio of the exterior to the interior solid angle is ½ (i.e. this will change for sources located on corners and edges). Equation (2) suffers from the well known non-uniqueness difficulty where the solution is not unique at the resonant frequencies of the equivalent interior problem (Wu, 2000). This issue can be overcome using the Burton and Miller formulation which combines Equation (2) with the derivative of this equation with respect to the receiver position $\mathbf{y}$ (Burton & Miller, 1971). The derivative equation takes the form:

$$-\frac{1}{2}\frac{\partial p(\mathbf{y})}{\partial n(\mathbf{y})} = \int_S \frac{\partial p(\mathbf{x})}{\partial n(\mathbf{x})} \frac{\partial G(\mathbf{x},\mathbf{y})}{\partial n(\mathbf{y})} dS(\mathbf{x}) - \int_S p(\mathbf{x}) \frac{\partial^2 G(\mathbf{x},\mathbf{y})}{\partial n(\mathbf{x}) \partial n(\mathbf{y})} dS(\mathbf{x}) \tag{3}$$

Denoting the normal derivative of surface pressure as q, the 1st and 2nd integrals in Equation (2) as $L(q)$ and $M(p)$ respectively and the corresponding integrals in Equation (3) as $L'(q)$ and $M'(p)$, the combined boundary integral equation is:

$$-\frac{1}{2}\left(p(\mathbf{y}) + \lambda q(\mathbf{y})\right) = (L + \lambda L')q(\mathbf{x}) - (M + \lambda M')p(\mathbf{x}) \tag{4}$$

where λ is the coupling parameter which will give a unique solution at all frequencies if set to a complex number (Liu, 2009). Here λ is set to $0.03i/k$, which is optimal for a range of k values (Gumerov, 2007). Equation (4) can be solved with appropriate boundary conditions (BCs) which will reduce the number of unknowns at $\mathbf{y}$ to 1. In particular, either the pressure or its normal derivative are known (corresponding to a Dirichlet or Neumann BC) or a linear relation is known between them (Robin BC).

The elastodynamic integral equation

The elastodynamic boundary integral equation can be derived using the dynamic reciprocal theorem, which can relate two distinct elastodynamic states or solutions throughout a body (Manolis & Beskos, 1988). Substitution of these states into the time-harmonic equation of motion, followed by subtraction of one equation from the other and integration of the result, yields an equation analogous to Green's second iden-

tity (Chaillat, 2008b). The two states can be chosen as the unknown state being solved for and the fundamental solutions for elastodynamic Navier equation (Mesquita & Pavanello, 2005). As with the Helmholtz Green's function, these fundamental solutions satisfy the Sommerfeld radiation condition and therefore ensure the corresponding BIEs also adhere to the same decay/radiation conditions at infinity (Mesquita & Pavanello, 2005). Again applying a limiting process to place all variables on the boundary gives the BIE:

$$\begin{aligned}\frac{1}{2}u_i(\mathbf{y}) &= -\int_S u_i(\mathbf{x})T_i^k(\mathbf{x},\mathbf{y};\omega)dS_y \\ &\quad +\int_S t_i(\mathbf{x})U_i^k(\mathbf{x},\mathbf{y};\omega)dS_y\end{aligned} \tag{5}$$

for the interior problem, where u_i and t_i are the ith components of displacement and traction (or surface stress) and the fraction again comes about from the surface being smooth at **y**. The elastodynamic fundamental solutions U and T describe the ith components of displacement and surface stress at the 'receiver' position **y** resulting from a unit point force applied at **x**, in the direction k (Bonnet, Chaillat & Semblat, 2009). These can be written in the form:

$$\begin{aligned}U_i^k(\mathbf{x},\mathbf{y};\omega) &= \frac{1}{k_S^2\mu}e_{qi}e_{skl}\frac{\partial}{\partial x_q}\frac{\partial}{\partial y_s}G_S(\mathbf{x},\mathbf{y}) \\ &\quad +\frac{1}{k_S^2\mu}\frac{\partial}{\partial x_q}\frac{\partial}{\partial y_s}G_P(\mathbf{x},\mathbf{y}) \\ T_i^k(\mathbf{x},\mathbf{y};\omega) &= C_{ijhl}\frac{\partial}{\partial y_l}U_h^k(\mathbf{x},\mathbf{y};\omega)n_j(\mathbf{y})\end{aligned} \tag{6}$$

where G_S and G_P are the Green's functions (Equation (1)) with wavenumbers corresponding to the transverse S waves and longitudinal P waves (Chaillat, Bonnet and Semblat, 2008). For shear modulus μ, Poisson's ratio ν and density ρ, these wavenumbers can be written as:

$$k_S^2 = \frac{\rho\omega^2}{\mu} \quad k_P = \gamma k_S \quad \gamma^2 = \frac{1-2\nu}{2(1-\nu)} \tag{7}$$

(Bonnet, Chaillat & Semblat, 2009). The fundamental solutions in Equation (6) also use the permutation symbol which may be written in terms of the kronecker delta function as $e_{qil}e_{skl} = \delta_{qs}\delta_{ik} - \delta_{qk}\delta_{is}$, as well as the 4th order elasticity tensor:

$$C_{ijhl} = \mu\left(\frac{2\nu}{1-2\nu}\delta_{ij}\delta_{hl} + \delta_{ih}\delta_{jl} + \delta_{jh}\delta_{il}\right) \tag{8}$$

which is only dependent on the material properties (Chaillat, Bonnet and Semblat, 2008). Again, suitable BCs are required to reduce the number of unknowns: a known surface stress corresponds to the Neumann BC while a Dirichlet condition corresponds to a known displacement (Chaillat, 2008).

COUPLED FLUID-STRUCTURE MODEL

To couple the Helmholtz (Equation (4)) and elastodynamic (Equation (5)) BIEs, a total of 4 equations need to be solved (the scalar Helmholtz equation and the 3 xyz components of the vector elastodynamic equation). These equations contain 8 unknowns in total (the fluid pressure and its normal derivative, the 3 components of structure displacement and the 3 components of surface stress), which can be reduced using the boundary conditions to yield a well posed system of equations. Continuity requirements at the boundary require the tangential components of surface stress to be 0 as fluids will not support shear stress. The surface stress vector **t** can then be related to the fluid pressure on the surface as:

$$\mathbf{t} = -p\mathbf{n} \tag{9}$$

for the outward pointing normal vector **n** (Gaul, Brunner & Junge, 2009). Continuity of displacement at the boundary relates the normal derivative of the surface pressure q to the displacement vector **u** at a point on the boundary as follows:

$$q = \rho\omega^2\mathbf{u}\cdot\mathbf{n} \tag{10}$$

where ρ and ω are the density and angular frequency in the fluid (Brunner, Junge & Gaul, 2009). These boundary conditions allow both the Helmholtz and elastodynamic BIEs to be expressed in terms of the pressure and displacement on the boundary, yielding a 'well posed' system of equations with as many equations as unknowns. For the problem of calculating the scattered acoustic field for an object exposed to an incident acoustic field, the BIEs can be re-arranged such that the unknowns are placed on one side of the equation, analogous to an **Ax** = **b** type matrix equation. Substituting Equation (9) and Equation (10) into Equation (5) and Equation (4) respectively, introducing an incident pressure field p^i on the right of Equation (4) (Wu, 2000) and rearranging yields:

$$\begin{aligned}p^i(\mathbf{y}) &= -\frac{1}{2}\Big(p(\mathbf{y}) + \lambda\rho\omega^2\mathbf{u}(\mathbf{y})\cdot\mathbf{n}(\mathbf{y})\Big) \\ &\quad -(L+\lambda L')\lambda\rho\omega^2\mathbf{u}(\mathbf{x})\cdot\mathbf{n}(\mathbf{x}) \\ &\quad +(M+\lambda M')p(\mathbf{x})\end{aligned} \tag{11}$$

$$\begin{aligned}0 &= \frac{1}{2}\mathbf{u}(\mathbf{y}) + \int_S \mathbf{u}(\mathbf{x})T^k(\mathbf{x},\mathbf{y};\omega)dS_y \\ &\quad +\int_S p\mathbf{n}(\mathbf{x})U^k(\mathbf{x},\mathbf{y};\omega)dS_y\end{aligned} \tag{12}$$

where the Cartesian component subscript has been dropped from Equation (12) such that the displacement vector appears explicitly in both equations. It should be understood that in these equations, the receiver position **y** refers to an arbitrary current 'centre' point for which the coupled pressure and displacement field is being solved, while the source position **x**, which only appears in the context of the boundary integrals, refers to the Green's function source position in *every* element. Equation (11) and (12) may be simultaneously solved using an iterative technique such as the generalised minimum residual (GMRES) method. GMRES has been shown to be the most efficient solver for acoustic problems (Marburg & Schneider, 2003) and has also been successfully utilised in coupled problems (Brunner, Junge & Gaul, 2009).

THE FAST MULTIPOLE METHOD

Iterative solution of the coupled system of equations requires the matrix-vector product between the discretised integral terms and the current iteration of the solution, at a cost of N^2 operations for a system of N unknowns. The FMM can significantly reduce this numerical cost by approximately calculating the matrix-vector multiplication, but to a prescribed accuracy (Gumerov & Duraiswami, 2009). The coefficient matrix is not explicitly formed (thus requiring substantially less memory than a BEM) nor directly multiplied (hence the reduction in algorithm complexity).

The key feature of the FMM is the representation of the Green's function (Equation (1)) as a 'factorised' solution, built from two multipole functions (in the form of series expansions), which describe the Green's function in a 'near' and 'far' field (Gumerov & Duraiswami, 2009). This separation introduces an intermediate point (or expansion centre) which allows the two multipole functions to be independently calculated. The expansion centres of the multipole functions can be shifted, or 'translated', using special operations and multipole functions with alike centres can be combined into a single series expansion. Shifts in the expansion centre also change the domains in which the multipole expansions are valid, allowing interactions between larger or smaller groups, or changes in the representation from the far to the near field (Gumerov & Duraiswami, 2009). The far field function describes the field radiated by a Green's function exterior to a sphere defined by the source position and expansion centre, while the near field function describes the field received at a point interior to a sphere, defined by the receiver location and the expansion centre. The translation operations are used for the far field expansions to shift to a larger sphere (i.e. domain of validity) to allow more elements in a larger region to be combined and represented as a single expansion. Conversely the near field translations can be used to reduce the sphere size to represent the field received by a smaller group of elements. The far to near translation serves to take the field radiated exterior to a sphere containing a group of sources and transforms this expansion to the received field inside another well separated sphere, for the group of receivers within.

This allows the integrals for groups of neighbouring elements to be represented to all other well separated groups as a single multipole function and so the FMM deals with interactions between groups of elements, instead of individual Green's functions. A comparison of the interactions in the BEM and FMBEM is shown in Figure 1. The summations of expansions are shown with circles of different sizes corresponding to larger domains (i.e. summations of larger regions of elements) which are only valid at larger separation distances. The translations from far to near field are shown only for the largest summations (from the white to black circles) where these operations are actually applied for all levels.

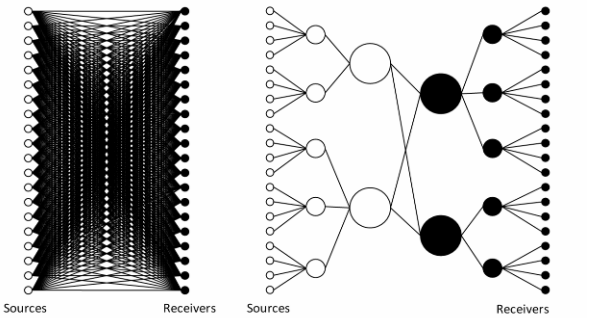

Figure 1. Comparison of direct interactions of Green's functions (left) and fast multipole interactions (right) (adapted from Gumerov and Duraiswami (2004)).

Thus to implement the FMM requires the following: multipole expansions which allow the factorised Green's function to be built, translation algorithms which can apply 'far to far', 'near to near' and 'far to near' type operations to the sets of individual/combined expansion coefficients and finally, a method to systematically define what is 'near' and 'far' in 3-dimensional space. Also, it should be noted that the requirement that the interactions between sources and receivers be 'well separated' means that the near field interactions, that is, the Green's function interactions between one boundary element and it's nearest neighbours, cannot be calculated using the FMM. When the technique is incorporated into the BEM, these interactions (which can be envisaged as the near/on diagonal coefficients of the corresponding BEM matrix) must be directly calculated using numerical quadrature, while the FMM deals with the other well separated interactions.

Multipole expansions of the Green's functions

There are a number of methods for deriving suitable series expansions to factorise the Green's function. The functions used here are derived from general solutions to the equations resulting from a separation of variables of the spherical Helmholtz equation. These general solutions take the form of Spherical Bessel functions, Legendre functions and complex exponentials (Gumerov & Duraiswami, 2004). The multipole expansions, referred to here as spherical basis functions, can be constructed from combinations of the general solutions which satisfy realistic conditions with respect to the limits of the spherical radial coordinate (at 0 and infinity). The two spherical basis functions are the near (or regular) R and far (or singular) S functions, whose names reflect whether the basis function is singular or regular when the expansion vector $\mathbf{r} = 0$. The R and S functions are:

$$R_n^m(\mathbf{r}) = j_n(kr)Y_n^m(\theta,\phi) \tag{13}$$

$$S_n^m(\mathbf{r}) = h_n(kr)Y_n^m(\theta,\phi) \tag{14}$$

where the expansion degree $n = 0, 1, 2, \ldots$ and order $m = -n, -n+1, \ldots, n-1, n$, k is the wavenumber, r, θ and ϕ are the radial distance, polar angle (measured from the positive z-axis) and azimuth angle (measured from the positive x-axis in the xy plane) of the spherical coordinate system and j and h are the spherical Bessel and spherical Hankel functions, both of the first kind (Gumerov & Duraiswami, 2004). The basis functions also use the spherical harmonic function:

$$\begin{aligned} Y_n^m(\theta,\phi) &= (-1)^m \sqrt{\frac{2n+1}{4\pi}\frac{(n-|m|)!}{(n+|m|)!}} \\ &\quad \times P_n^{|m|}(\cos\theta)e^{im\phi} \end{aligned} \tag{15}$$

where P is the associated Legendre function (Epton & Dembart, 1995). The S and R basis functions can be combined to build the free space Green's function (Equation 1) as:

$$\begin{aligned} G(\mathbf{r}_1+\mathbf{r}_2) &= ik\sum_{n=0}^{\infty}\sum_{m=-n}^{n} S_n^{-m}(-\mathbf{r}_1)R_n^m(\mathbf{r}_2) \\ &= ik\sum_{n=0}^{\infty}\sum_{m=-n}^{n} R_n^{-m}(-\mathbf{r}_2)S_n^m(\mathbf{r}_1) \end{aligned} \tag{16}$$

with $|\mathbf{r}_2| < |\mathbf{r}_1|$ (Gumerov & Duraiswami, 2004). In Equation (16), the 2 vectors are defined in terms of the source and receiver location and the intermediate expansion centre. The BIEs of interest involve both the normal surface derivative and mixed partial derivatives of the Green's function. These can be obtained for the S and R expansions by applying the Cartesian partial derivatives to the corresponding Bessel/Hankel functions. More interestingly, it has been shown that by employing various recursion relations for those functions, the normal/partial derivatives of the basis functions can be expressed in terms of combinations of the same S and R functions with shifts in the degree and order of expansion (Gumerov & Duraiswami, 2003).

Translations of the *S* and *R* basis functions

To numerically implement the FMM, the *S* and *R* basis functions are truncated with a suitable number of terms dictated by the allowed error for the solution. For a multi-level FMM as indicated in Figure 1, the number of terms used on each level must vary to reduce the algorithm complexity, usually proportional to both the wavenumber and the size of the domain for which the expansions are valid. A number of methods are available for the selection of the truncation number, for example using empirical relations (Darve, 2001; Liu, 2009) or based on asymptotic error limits and a prescribed accuracy for the FMM (Gumerov & Duraiswami, 2009).

As a result, an expansion truncated with a degree = p will have p^2 degree and order combinations to translate. Furthermore, translations applied between FMM levels with different truncation numbers will require a mechanism to transform the expansions to similar lengths, to combine them. Replacing the terminology 'near' and 'far' with the *R* and *S* expansions respectively gives the 3 types of translation as $R|R$, $S|S$ and $S|R$ type operations. For all cases, the operations allow a new vector to translate an existing set of expansions and the result will be the corresponding *S* or *R* basis functions of the original expansion vectors, plus the new translation vector. The equations describing these translations are:

$$R_n^m(\mathbf{r}+\mathbf{t}) = \sum_{n'=0}^{\infty}\sum_{m'=-n'}^{n'}(R\mid R)_{n'n}^{m'm}(\mathbf{t})R_{n'}^{m'}(\mathbf{r}) \quad (17)$$

$$S_n^m(\mathbf{r}+\mathbf{t}) = \sum_{n'=0}^{\infty}\sum_{m'=-n'}^{n'}(S\mid S)_{n'n}^{m'm}(\mathbf{t})S_{n'}^{m'}(\mathbf{r}) \quad (18)$$

$$S_n^m(\mathbf{r}+\mathbf{t}) = \sum_{n'=0}^{\infty}\sum_{m'=-n'}^{n'}(S\mid R)_{n'n}^{m'm}(\mathbf{t})R_{n'}^{m'}(\mathbf{r}) \quad (19)$$

where the $S|R$ and $S|S$ operators are valid for $|\mathbf{r}| < |\mathbf{t}|$ and $|\mathbf{r}| > |\mathbf{t}|$ respectively and the 2 sets of degree and order coefficients have the same range as the spherical basis functions (Gumerov & Duraiswami, 2009). Assuming a truncated expansion with p^2 terms, the 'best' algorithm for applying the translation will be of the order of p^2 operations (one operation per coefficient). Practically, the algorithms which apply the translations do not reach this limit, with the original implementation requiring the order of p^4 operations (Greengard & Rokhlin, 1988). A number of faster algorithms are available: the one implemented here is referred to as the rotation, coaxial translation, rotation algorithm (RCR algorithm), details for which can be found in, for example, Gumerov and Duraiswami (2004). Both rotating the coordinate system as well as applying a translation along the z-axis, have a complexity of the order of p^3 operations when conducted using recursion relations. Thus the RCR algorithm rotates the set of expansion coefficients such that the translation vector is along the z-axis of the new coordinate system, applies the z-axis translation and then rotates the coordinate system back.

The RCR translation algorithm is in fact a 'low frequency' algorithm which is suited to applying translations for smaller groups of elements (i.e. with a smaller number of wavelengths across the group). For larger groups of elements, where there are many wavelengths across the sphere containing the set of expansion vectors, the number of expansion terms required to represent the set of sources and receivers must increase. The RCR algorithm complexity significantly slows down the FMM as the number of operations per translation increases (the majority of the computational work in the FMM procedure results from the $S|R$ translations). Hence the 'broadband' type FMM implementations mentioned in the introduction apply a switch in the translation method when the spherical domain containing a set of expansions reaches a certain size (measured in terms of the number of wavelengths across the group). These high frequency translation methods (again, there are many types available) have a lower algorithmic cost and so the overall FMM algorithm complexity is minimised. Unfortunately, the high frequency algorithms are unstable at lower frequencies and this precludes their exclusive use in the FMM algorithm. Finally, it should be noted that the RCR algorithm incorporates procedures to change the length of the expansions for $R|R$ and $S|S$ type operations.

The octree structure

The FMM requires a method for determining what is 'near' and 'far' from an element on an arbitrary boundary element mesh in 3-dimensional space, to both allow nearby elements to be represented with a single basis function (with respect to a common expansion centre) and ensure the domains of validity for the expansions are respected. This structured division can be achieved via the octree structure, which is applied to an arbitrary set of points (such as the centres of plane triangular elements which coincide with the source positions), normalised to the unit cube (Gumerov & Duraiswami, 2004).

The unit cube (referred to as level 0) is subdivided into 8 smaller cubes (level 1), which are similarly subdivided and the process repeated to an arbitrary level of division. An octree structure for a spherical boundary mesh at different levels of subdivision is shown in Figure 2 below.

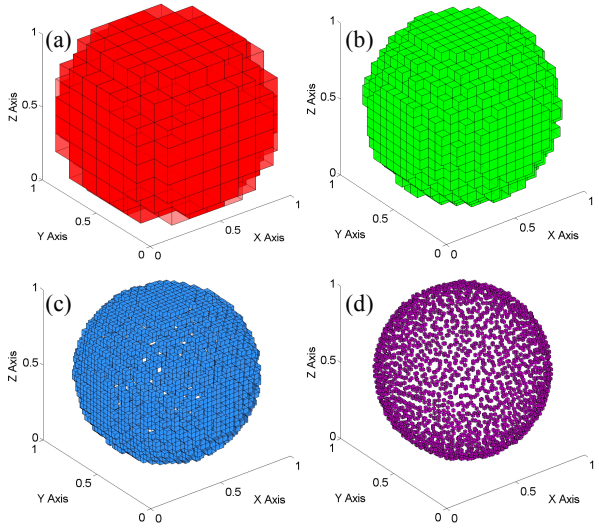

Figure 2. Octree structure for a spherical boundary element mesh at different octree levels. Subfigure (a), (b), (c) and (d) correspond to octree levels 3, 4, 5 and 6 respectively. The sources for the elements are contained within the cubes.

Each cube, or box, on each level of the octree has a 'box number' associated with it and these numbers identify what region of space the box bounds. For any box, the larger containing box is referred to as the parent, while the 8 smaller boxes resulting from subdivision are the children and the surrounding boxes (sharing a common edge or vertex) are the neighbours (Gumerov, Duraiswami & Borovikov, 2003). For an arbitrary set of normalised points, box numbers can be associated with the set by constructing a bit-interleaved integer from the Cartesian coordinates of each point. The box number is constructed by converting the decimal coordinates of the points into integers and then interleaving the corre-

sponding binary strings into a single binary number. The interleaved string is constructed by taking the leading bit of each of the xyz coordinate integers and combining them into a 3-bit group, then combining the second most significant bits and concatenating this group onto the binary string, and so on (Gumerov, Duraiswami & Borovikov, 2003). Each 3-bit binary group corresponds to an integer between 0 and 7 which indicates (from the most significant group) which of the 8 boxes the point occupies on level 0, with the next 3-bit group indicating the child box occupied by the point (i.e. the successive box on level 2) and so forth (Gumerov, Duraiswami & Borovikov, 2003). Thus an octree with l levels can truncate the box numbers after $3l$ bits of the bit interleaved string.

The octree structure provides a fast method of determining if a group of points are near to one another, as all points occupying a particular box will have the same box number (determined by the leading $3l$ bits of any level l). Search operations to determine the parent or children of a box can be calculated using bit-shift operations while the list of possible neighbours and the coordinates of the cube centre can be determined by deinterleaving the binary box number (Gumerov, Duraiswami & Borovikov, 2003). Hence the octree structure provides fast methods to determine the relations pertinent to the FMM (near and far fields as well as parent/child search operations) which do not require searches through lists of coordinates. Furthermore, as the boxes are built from the data positions, empty boxes are never created.

Matrix-vector multiplication via the FMM

In this section, the procedure for conducting a matrix-vector multiplication using the FMM is discussed. The matrix is assumed to be composed of the Green's function coefficients for a BIE and the vector represents the current solution vector in an iterative solution. Each of the Green's function coefficients represents an integral over a boundary element at the receiver position due to the radiating Green's function source (in fact each source contributes to every other receiver and vice versa). The aim of the iterative solution is to determine the 'strengths' of the Green's functions (i.e. the surface total pressure and the displacement field). For the numerical discretisation implemented here, the elements used are plane triangular elements and the sources and receivers are made coincident at the centre of each element.

The FMM only provides a means to calculate the Green's functions while the BEM requires integrals of kernels involving them. In the far field (the elements outside of the receiver box and its neighbouring boxes), the sources are suitably separated to be represented using multipole expansions. As the Green's function is dependant on the radial distance, at large distances there will be little variation of the Green's function over the elements and so the integrals can be approximated as the Green's function multiplied by the element area (Gumerov & Duraiswami, 2009). In the near field the sources of the near elements are not far enough away to allow multipole representations and so the integrals of these elements must be directly included (i.e. using low order Gaussian quadrature). The FMM integration is incorporated by simply multiplying the source strengths by the element areas at the start of the procedure while the near field is included in the final step. Using the standard terminology, the FMM consists of an upward and a downward pass as follows:

1. Calculate the far field expansions for each source on the lowest level of the octree structure with respect to a common expansion centre (the box centre) and combine into a single set for each box. Note that because the $S|R$ translations in Equation (20) act on regular R expansions and yield the far field S expansions, Equation (14) is used to build the far field representations and Equation (15) is not used explicitly.

2. *Upward Pass*: For each octree level, apply $S|S$ translations from the children boxes to the centre of the parent box and combine into a single expansion set. Of course, as these expansions are actually R expansions, the $R|R$ operation should be used. It has been shown that the 2 translation operations are in fact the same and only depend on the basis function being translated (Gumerov & Duraiswami, 2004). Summations are built for every box up to level 2 (a 4x4x4 subdivision), the highest level for which the boxes have a well separated far field (Gumerov, Duraiswami & Borovikov, 2003). The upward pass builds a basis function representation for all the sources contained with every box on each level of the octree structure as a single combined set of expansion coefficients. Figure 3 below shows a spherical mesh and the corresponding expansion/translation vectors for 2 octree levels.

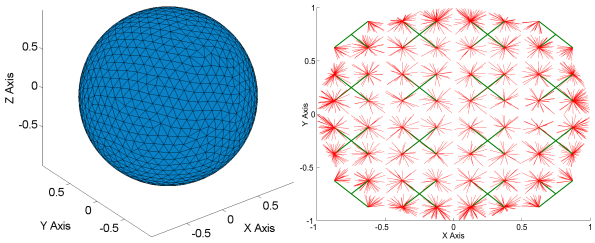

Figure 3. Boundary element mesh of a sphere and the corresponding R expansions (red lines) between the source positions (the centre of each element) and the centre of the box. The translation vectors (green lines) are from the child to the parent box centres. Note that the 3-dimensional vectors are shown along an axis direction to show the vectors in a plane.

3. *Downward Pass*: In this stage, the far field results for each receiver are calculated by applying the $S|R$ translations to all boxes in the far field (i.e. excluding any elements in the receiver box and its neighbours). Starting at level 2, all R expansions for the far field boxes are $S|R$ translated to the centre of each box (yielding S expansions in accord with Equation (20)). These are then $S|S$ translated back down the octree to each of the children boxes (on octree level 3). On this level there will now be boxes which reside in the far field (as the separation distance has reduced with respect to the smaller boxes) whose contributions were not included in the level 2 $S|R$ translations. Formally, the additional far field region revealed on successive octree levels is the current boxes' parents' neighbours' children boxes, minus the near field of the box, totalling at most 189 $S|R$ translations (Greengard et al, 1998). These new contributions to the far field multipole expansion are added to the current set of S expansions and the process repeated down to the lowest level. Figure 4 shows the far field boxes and corresponding $S|R$ translation vectors for an arbitrary receiver box for a 2 level octree.

4. At the lowest octree level, the final set of expansions describes the radiated field from all far boxes. The total far field can be evaluated at each of the receiver points by applying Equation (17) for the combined far field S expansions and the receiver R expansions (from the receiver box centre to the receiver point at the centre of each plane triangle element). The near field is calculated using gauss quadrature and special techniques are used to treat the near singular and singular behaviour of the Green's function as the radial distance tends to 0 (Scudder, 2007). The final result is the complete field from the numerical integrals over the boundary, at each of the receiver points.

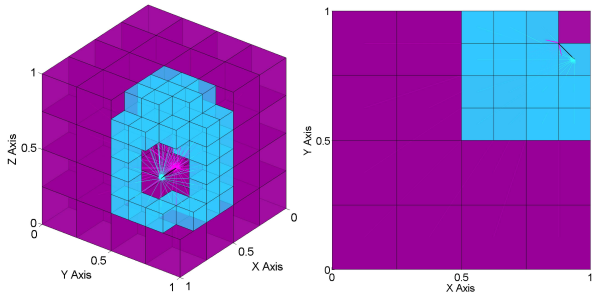

Figure 4. The far field boxes and $S|R$ translations for a receiver box in a 2 level octree. The purple boxes and vectors are the far boxes and $S|R$ translation from level 2 of the octree. The black vector is the $S|S$ translation to the lower octree level. The blue boxes/vectors indicate the new far field region which can now be included on the lower octree level.

ACOUSTIC FMBEM RESULTS

An acoustic FMBEM code has been developed in MATLAB which implements the FMM procedure presented in the previous section. Examples of FMBEM results are presented here for the segmented BeTSSi rigid submarine model (Nell & Gilroy, 2003). Figure 5 compares the FMBEM total surface pressure to that from a commercial software package (PAFEC) for a unit strength plane wave source at a broadside angle and a frequency of 200Hz. The relative norm of the residuals of the 2 solutions is 9%, with the largest observed discrepancies at the back of the fins where the mesh is the thinnest. The PAFEC results on these regions are not smoothly varying and do not improve as the mesh is refined, suggesting the issue is with how the near singular integrals are calculated. Removal of 75 of the edge elements showing suspect pressures in the PAFEC results reduces the relative norm of the residuals between the solutions to 3%.

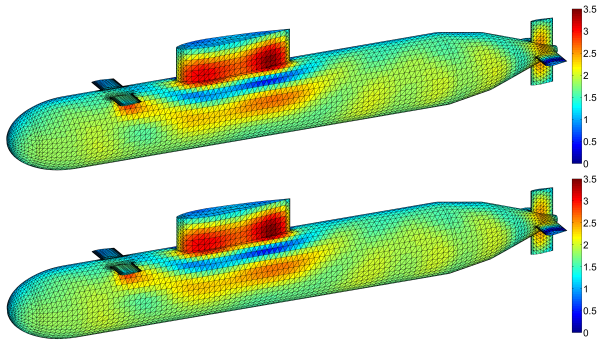

Figure 5. Total acoustic field for the segmented BeTSSi submarine for the FMBEM (top) and PAFEC (bottom) from a 200Hz plane wave source, broadside incidence. The pressure range for both plots is 0 to 3.5 Pa.

Figure 6 shows the monostatic target strength (TS) as a function of backscattered angle for the segmented BeTSSi submarine hull, as calculated by the acoustic FMBEM code as well as the PAFEC software (at 10° increments). Also included are the TS results for the original BeTSSi submarine model. The segmented BeTSSi model has a slightly different shape as it was constructed from simple geometric shapes to approximate the BeTSSi submarine model. These differences in the model should account for the differences in the results predicted by Avast. The TS results from the FMBEM and PAFEC (which use the same model) show good agreement.

The BeTSSi model in Figure 5. consists of 14640 elements which appears to be in the upper echelon of problem sizes that PAFEC can solve. Comparatively, the FMBEM code solved the problem about 12 times faster using approximately 14 times less memory. Here the moderate performance of the FMBEM code can be attributed in part to the large variation in element sizes, for which an adaptive FMM is superior.

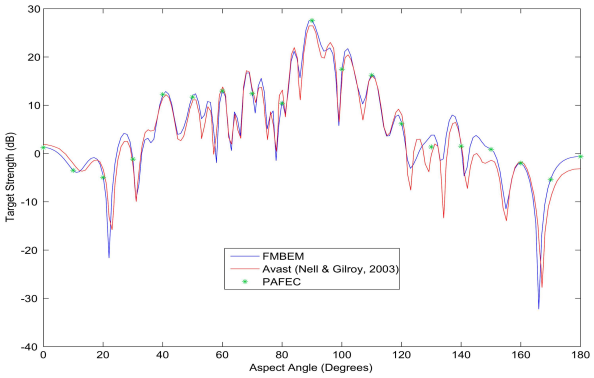

Figure 6. Monostatic target strength as a function of angle for the BeTSSi submarine at a frequency of 200Hz.

The reduced computational and memory requirements of the FMBEM allow large problems with many unknowns to be solved on desktop PCs. A refined model of the segmented BeTSSi submarine with 331 039 elements was solved at a similar frequency in approximately 3 hours on an i7 processor with 12Gb of RAM. The equivalent matrix-vector multiplication of each of the full BEM matrices would require 1.09 $x10^{11}$ operations and 1753Gb of space to store. These results are atypical of the competitive FMM algorithms presented in many of the references which are *at least* an order of magnitude faster, due to their use of advanced FMM techniques not yet incorporated into the code, as well as the choice of faster programming languages. Computationally intensive parts of the code will be rewritten in C and called by the central MATLAB program, thus allowing the code to easily incorporate multi-threaded and GPU acceleration via MATLAB.

CONCLUSIONS AND FURTHER WORK

A numerical method has been proposed for modelling coupled fluid-structure interactions using a fast multipole accelerated BEM for both the fluid and structure, where coupling is achieved via enforcing continuity of pressure and displacement on the common boundary. Currently, an acoustic FMBEM program has been completed which is providing a significant increase in performance compared to a traditional commercial BEM code. Further improvements to the current code, chiefly, the incorporation of a high frequency translation technique, will substantially increase its performance. Current work is focused on developing the elastodynamic FMBEM based on the acoustic code. Finally, the proposed coupled FMBEM-FMBEM model will be investigated.

REFERENCES

Amini, S, Harris, PJ & Wilton, DT 1992, *Coupled Boundary and Finite Element Methods for the Solution of the Dynamic Fluid-Structure Interaction Problem*, Lecture Notes in Engineering no. 77, Springer-Verlag.

Amini, S & Profit ATJ 2003, 'Multi-level Fast Multipole Solution of the Scattering Problem', *Engineering Analysis with Boundary Elements*, vol. 27, pp. 547-564.

Beskos, DE 2003, 'Dynamic Analysis of Structures and Structural Systems', in Beskos, D & Maier, G, *Boundary Element Advances in Solid Mechanics*, CISM Courses and Lectures no. 440, SpringerWienNewYork, Italy.

Bonnet, M, Chaillat, S & Semblat, JF 2009, 'Multi-Level Fast Multipole BEM for 3-D Elastodynamics', in GD Manolis & D Polyzos (ed.), *Recent Advances in Boundary Element Methods*, Springer, pp. 15-27.

Brunner, D, Junge, M & Gaul, L 2009, 'A comparison of FE-BE coupling schemes for large-scale problems with fluid-structure interaction', *International Journal for Numerical Methods in Engineering*, no. 77, pp. 664-688.

Brunner, D, Of, G, Junge, M, Steinbach, O & Gaul, L 2009, 'A fast BE-FE coupling scheme for partly immersed bodies', *International Journal for Numerical Methods in Engineering*, vol. 81, no. 1, pp. 28-47.

Burton, AJ & Miller, GF 1971, 'The application of integral equation methods to the numerical solution of some exterior boundary-value problems', *Proceedings of the Royal Society of London. Series A, Mathematical and Physical Sciences*, vol. 323, pp. 201-210.

Chaillat, S, Bonnet, M & Semblat, JF 2008, 'A multi-level fast multipole BEM for 3-D elastodynamics in the frequency domain', *Computational Methods in Applied Mechanics and Engineering*, no. 198, pp. 4233-4249.

Chaillat, S 2008, 'Fast Multipole Method for 3-D elastodynamic boundary integral equations. Applications to seismic wave propagation.', PhD Thesis, Ecole Polytechnique, Paris.

Chaillat, S, Bonnet, M & Semblat, JF 2009, 'A new fast multi-domain BEM to model seismic wave propagation and amplification in3-D geological structures', *Geophysical Journal International*, vol. 177, pp. 509-531.

Cheng, H, Crutchfield, WY, Gimbutas, Z, Greengard, LS, Ethridge, JF, Juang, J, Rokhlin, V, Yarvin, N & Zhao, J 2006, 'A wideband fast multipole method for the Helmholtz equation in three dimensions', *Journal of Computational Physics*, vol. 216, pp. 300-325.

Coifman, R, Rokhlin, V & Wandzura, S 1993, 'The Fast Multipole Method for the Wave Equation: A Pedestrian Prescription', *IEEE Antennas and Propagation Magazine*, vol. 35, no. 3, pp. 7-12.

Epton, MA and Dembart, B, 'Multipole Translation Theory for the Three-Dimensional Laplace and Helmholtz Equations', *SIAM Journal of Scientific Computing*, vol. 16, no. 4, pp. 865-897.

Darve, E 2000, 'The fast multipole method I: Error analysis and asymptotic complexity', *SIAM Journal of Scientific Computing*, vol. 38, no. 1, pp. 98-128.

Fischer, M & Gaul, L 2005, 'Fast BEM-FEM mortar coupling for acoustic-structure interaction', *International Journal for Numerical Methods in Engineering*, no. 76, pp. 2137-2156.

Fujiwara, H 2000, 'A fast multipole method for solving integral equations of three-dimensional topography and basin problems', *Geophysical Journal International,* vol. 140, pp. 198-210.

Gaul, L, Brunner, D & Junge, M 2009, 'Simulation of Elastic Scattering with a Coupled FMBE-FE Approach' in GD Manolis & D Polyzos (ed.), *Recent Advances in Boundary Element Methods*, Springer, pp. 131-145.

Greengard, L & Rokhlin, V 1988, *On the Efficient Implementation of the Fast Multipole Algorithm*, Department of Computer Science, Yale University

Greengard, L, Huang, J, Rokhlin, V and Wandzura, S 1998, 'Accelerating Fast Multipole Methods for the Helmholtz equation at Low Frequencies', *IEEE Computational Science and Engineering*, vol. 5, no. 3, pp. 32-38.

Gumerov, NA & Duraiswami, R 2003, 'Recursions for the Computation of Multipole Translation and Rotation Coefficients for the 3-D Helmholtz Equation', *SIAM Journal of Scientific Computing*, vol. 25, no. 4, pp. 1344-1381.

Gumerov, NA, Duraiswami, R & Borovikov, EA 2003, *Data Structures, Optimal Choice of Parameters, and Complexity Results for Generalized Multilevel Fast Multipole Methods in d Dimensions*, Institute for Advanced Computer Studies, University of Maryland.

Gumerov, NA & Duraiswami, R 2004, *Fast Multipole Methods for the Helmholtz Equation in Three Dimensions*, A Volume in the Elsevier Series in Electromagnetism, Elsevier, Oxford.

Gumerov, NA & Duraiswami, R 2007, *Fast Multipole Accelerated Boundary Element Methods for the 3D Helmholtz Equation*, Department of Computer Science and Institute for Advanced Computer Studies, University of Maryland.

Gumerov, NA & Duraiswami, R 2009, 'A broadband fast multipole accelerated boundary element method for the three dimensional Helmholtz equation', *The Journal of the Acoustical Society of America*, vol 125, no. 1, pp. 191-205.

Jensen, FB, Kuperman, FA, Porter, MB & Schmidt, H 2000, *Computational Ocean Acoustics*, Springer, New York.

Junger, MC & Feit, D 1993, *Sound, Structures and Their Interaction*, Acoustical Society of America.

Koc, S & Chew, C 1998, 'Calculation of acoustical scattering from a group of scatters', *The Journal of the Acoustical Society of America*, vol. 103, no. 2, pp.721-734.

Liu, Y 2009, *Fast Multipole Boundary Element Method: Theory and Applications in Engineering*, Cambridge University Press, New York.

Manolis, GD & Beskos, DE 1998, *Boundary Element Methods in Elastodynamics*, Unwin-Hyman, London.

Marburg, S, Schneider, S 2003, 'Performance of iterative solvers for acoustic problems. Part 1. Solvers and effect of diagonal preconditioning', *Engineering Analysis with Boundary Elements*, no. 27, pp. 725-750.

Masumoto, T, Gunawan, A, Oshima, T, Yasuda, Y & Sakuma, T 2008, 'Coupling analysis between FMBEM-based acoustic and modal-based structural models', *Proceedings of the 37th International Congress and Exposition on Noise Control Engineering*, Shanghai, China.

Mesquita, E & Pavanello, R 2005, 'Numerical Methods for the dynamics of unbounded domains', *Computational & Applied Mathematics*, vol. 24, no. 1, pp. 1-26

Nell, CW & Gilroy, LE 2003, *An Improved BASIS Model for the BeTSSi Submarine*, DRDC Atlantic, Defence Research and Development Canada.

Reddy, JN 2004, *An Introduction to Nonlinear Finite Element Analysis*, Oxford University Press, New York.

Rokhlin, V 1990, 'Rapid Solution of Integral Equations of Scattering Theory in Two Dimensions', *Journal of Computational Physics*, vol. 86, no. 2, pp. 414-439.

Schneider, S 2008, 'FE/FMBE Coupling to fluid-structure interaction', *International Journal for Numerical Methods in Engineering*, no. 76, pp. 2137-2156.

Scuderi, L 2008, 'On the computation of nearly singular integrals in 3D BEM collocation', *International Journal of Numerical Methods in Engineering*, no. 78, pp. 1733-1770

Wu, TW 2000, 'The Helmholtz integral equation' in T Wu (ed.), *Boundary Element Acoustics: Fundamentals and Computer Codes*, Advances in Boundary Elements Series, WIT Press, Great Britain.

Xiao, H & Chen, Z 2007, 'Numerical experiments of preconditioned Krylov subspace methods solving the dense non-symmetric systems arising from BEM', *Engineering Analysis with Boundary Elements*, vol. 31, pp. 1013-1023.